

Unbiased Mean Teacher for Cross Domain Object Detection

Jinhong Deng¹ Wen Li¹ Yuhua Chen² Lixin Duan¹

¹University of Electronic Science and Technology of China ²Computer Vision Lab, ETH Zurich

jhdeng@std.uestc.edu.cn, {liwenbnu, lxduan}@gmail.com, yuhua.chen@vision.ee.ethz.ch

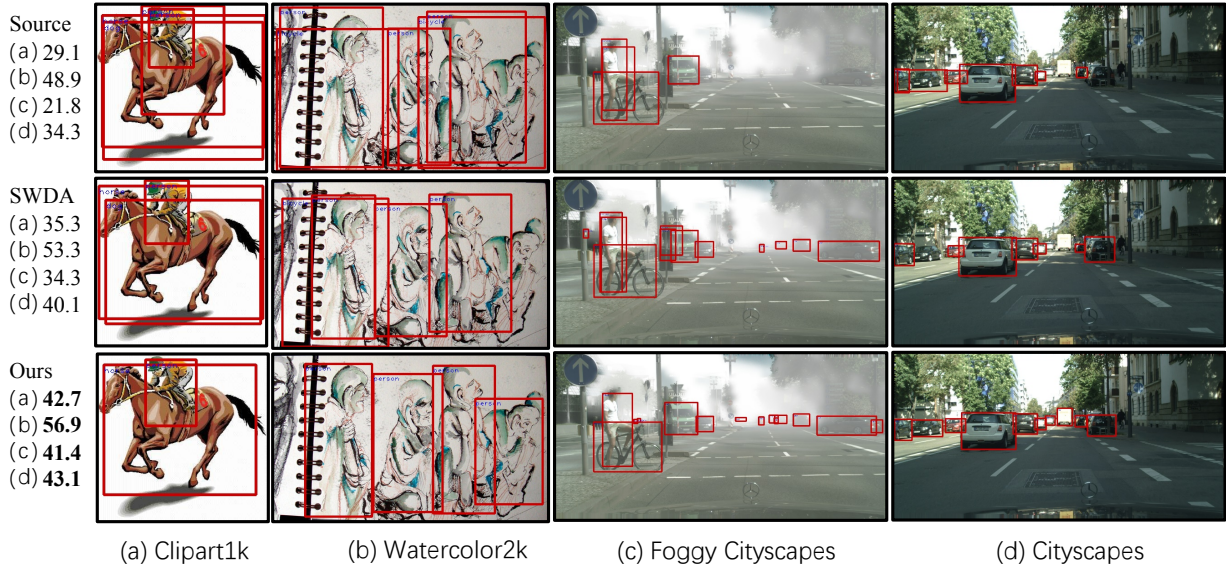


Figure 1: A comparison of different approaches for cross domain object detection, *top*: source only(no adaptation), *middle*: state-of-the-art method SWDA [32], *bottom*: our UMT approach. The mean average precision (mAP) on the four datasets are listed on the left side of each row. Our approach clearly outperforms others both qualitatively and quantitatively.

Abstract

Cross domain object detection is challenging, because object detection model is often vulnerable to data variance, especially to the considerable domain shift in cross domain scenarios. In this paper, we propose a new approach called Unbiased Mean Teacher (UMT) for cross domain object detection. While the simple mean teacher (MT) model exhibits good robustness to small data variance, it can also become easily biased in cross domain scenarios. We thus improve it with several simple yet highly effective strategies. In particular, we firstly propose a novel cross domain distillation for MT to maximally exploit the expertise of the teacher model. Then, we further alleviate the bias in the student model by augmenting training samples with pixel-level adaptation. The feature level adversarial training is also incorporated to learn domain-invariant representation. Those strategies can be implemented easily into MT and leads to our unbiased MT model. Our model surpasses the existing state-

of-the-art models in large margins on benchmark datasets, which demonstrates the effectiveness of our approach.

1. Introduction

In recent years, deep domain adaptation has gained increasing attention in computer vision community, because that the supreme performances achieved by deep models are normally only restricted in the domain of training data. When those trained models are applied to new environments, significant performance drops have often been observed in various computer vision tasks [4, 5, 9, 32, 47].

In this work we are specifically interested in the cross domain object detection problem, due to observing the strong demands from real world scenarios. For instance, in autonomous driving, robust object detection is needed in different weather and lighting conditions. Collecting annotation for all conditions can be extremely costly, and therefore models that can adapt to new environments without labeled

data are highly desirable.

Designing such domain adaptive detection models can be challenging. Compared to the image classification task, the output of object detection is richer and more complex, consisting of both the class labels and the bounding box locations. The two outputs are intrinsically coupled, making it more vulnerable towards data variance like scene change, weather conditions, camera diversity, *etc.* Various approaches have been proposed to address such issue, including instance and image level adversarial training [5], strong and weak adversarial training [32], graph based consistency [1], *etc.*

In this paper, we propose a new approach called Unbiased Mean Teacher (UMT) for cross domain object detection. We build our approach based on the mean teacher (MT) model [40], which is originally proposed for semi-supervised learning. By enforcing the consistency over perturbed unlabeled samples between the teacher and student models via distillation, it naturally gains improved robustness against data variance to some extent, and thus being used as our starting point for cross domain object detection. However, in the presence of a large domain gap, the MT model can be easily biased towards the source domain, as the supervision is mainly from source domain.

To overcome such model bias occurred in the mean teacher model for cross domain object detection, we design the unbiased mean teacher model with three strategies. Firstly, observing the biased teacher model often produce more precise prediction for the source images, we design a cross domain distillation approach by using the source-like target images translated with CycleGAN [48] as the input for teacher model, and original target images as the input for student model. This significantly improves the effectiveness of distillation. Then, to further remedy the model bias of student model, we use the target-like source images as additional labeled data for training. Finally, we incorporate feature level adversarial training into the student network for learning domain-invariant representation.

We extensively evaluate the proposed UMT model on several benchmarks, including PASCAL VOC to Clipart1k, PASCAL VOC to Watercolor2k, Cityscapes to Foggy Cityscapes and SIM10k to Cityscapes. Our new model achieves new state-of-the-art performance on all benchmarks by surpassing existing methods by large margins, demonstrating the effectiveness of the proposed model.

2. Related Works

Unsupervised Domain Adaptation: Unsupervised domain adaptation methods are designed to adapt a model from labeled source domain to an unlabeled target domain. Many previous works aim to minimize the distance metric such as maximum mean discrepancy(MMD)[3, 25, 26, 27, 39]. Alternatively, adversarial training with domain

classifier is also commonly used to learn domain-invariant representation [8, 9, 34, 42]. More similar to our work, French *et al.* proposed a model based on the Mean Teacher model [40], and achieved state-of-the-art results on various benchmarks. Their model includes student and teacher models. The student model is trained using gradient descent while the weights of the teacher network are an exponential moving average of those of the student, and the inconsistency in predictions between the two models is penalized to encourage model robustness. The aforementioned domain adaptation models have focused on the task image classification, while in this work we study a more challenging object detection problem.

Object Detection: Powered by the strong representation power of deep convolution neuron network(DCNN) models[14, 21, 38], object detection has made a significant progress in recent years. Many DCNN-based methods have been proposed [2, 10, 11, 13, 30, 28, 24, 29, 36, 22, 43], achieving remarkable performance in benchmarks such as PASCAL VOC[6] and MSCOCO[23]. Among all works, one of the most representative works is Faster RCNN [30], which first extracts regions of interest(RoIs) by a Region Proposal Network(RPN) and then the prediction is made based on the feature sampled from the RoI. In this work, we test our model using Faster RCNN [30] as our base detection network. But other detection network should also be possible.

Cross Domain Object Detection: Recently, many works have been proposed to address the domain shift problem occurred in object detection, using different techniques. DA-Faster [5] proposed two components for image-level and instance-level alignment respectively. SCDA [49] introduced a model which focuses on aligning the discriminative regions. MTOR [1] performs Mean Teacher[40] to explore object relation in region-level consistency, inter-graph consistency and intra-graph consistency. SWDA [32] utilizes strong and weak domain classifiers to align local and global features separately. A hierarchical domain feature alignment module is used in MAF [15] and [44] propose to align features across layers. Pixel-level adaptation have also been explored for the task of cross domain object detection. In more details, Shan *et al.* [35] employs generative adversarial network and the cycle consistency for image translation in the pixel space and minimize domain discrepancy in features. While DM [20] assumes that numerous shifted domain preserves the semantic information of the source domain but present differently. It first yields multiple domains from source and employs multi-domain-invariant representation learning. SPLAT [41] transforms the image using CycleGAN [48] alignment to conduct pixel-level adaptation and introduces paired alignment module between source and target detector that take adapted images as input. Besides, label-level adaptation [18, 19, 31] has also been used

for the task and yield improved detection performance. Our proposed Unbiased Mean Teacher model achieves improvements in large margins over the above methods.

3. The Unbiased Mean Teacher Model

In this section, we start from the mean teacher (MT) model [40], and discuss how to repurpose it for cross domain object detection. A simple MT model is firstly introduced by applying MT to object detection in a straightforward way. Then, we given an analysis on the model bias problem of MT model in the cross domain object detection task. Based on our analysis, we address the model bias in teacher model and student model respectively, and finally present our unbiased mean teacher model for cross domain object detection.

3.1. The Mean Teacher Model

Mean Teacher(MT) [40] was initially proposed for semi-supervised learning. It consists of two networks with identical architecture, a student model and a teacher model. The student model is trained using the labeled data as standard, and the teacher model uses the exponential moving average(EMA) weights of the student model. Each sample prediction of the teacher model can be seen as an ensemble of the student model’s current and earlier versions, therefore it is more robust and stable. By enforcing the consistency of teacher and student models using a distillation loss based on unlabeled samples, the student model is then guided to be more robust. The MT model has also been extended to unsupervised domain adaptation by using the target domain samples as the unlabeled data for distillation in [7].

During the distillation, a small perturbation is added to the unlabeled data. By selecting samples with high confidence for prediction, the student model is encouraged to learn more abstract invariances on the unlabeled target samples, thus further enhancing the model robustness. Therefore it is suitable to be applied to object detection, for addressing the issue that object detection model is sensitive to data variance due to simultaneously predicting the tangled bounding boxes and object classes.

However, since the mean teacher did not explicitly address the domain shift problem, when applying the MT model to the cross domain object detection task, the considerable domain shift might cause the predictions from teacher model unreliable, making the distillation less effective (see our investigation in Section 3.3). The recent work [1] proposes to use the region graph to facilitate the distillation, however, it still did not directly address the intrinsic model bias of the mean teacher model. Next, we will start from a simple MT model for cross domain object detection, and then discuss how to effectively deal with the model bias using domain adaptation strategies.

3.2. A Simple MT Model for Object Detection

In cross domain object detection task, we have a set of source images annotated with object bounding boxes and their class labels, and a set of unlabeled target images. The task is to learn a model to perform object detection in the target domain.

Formally, let us denote a source image as \mathbf{I}^s . An image is usually annotated with multiple bounding boxes as well as their class labels. We denote $\mathcal{B} = \{B_j|j=1\}^M$ as the set of bounding box coordinates with each $B_j = (x, y, w, h)$ representing a bound box. Accordingly, we denote by $\mathcal{C} = \{c_j|j=1\}^M$ as the corresponding class labels, in which each $c_j \in \{0, 1, \dots, C\}$ corresponds to B_j where 0 stands for background, the others for object class, and C is the total number of classes. Then the source domain can be represented as $\mathcal{D}_s = \{(\mathbf{I}_i^s, \mathcal{B}_i^s, \mathcal{C}_i^s)|i=1\}^{N_s}$, with N_s being the number of source images.

Similarly the target domain can be defined as $\mathcal{D}_t = \{\mathbf{I}_i^t|i=1\}^{N_t}$ where N_t is the number of target images.

Following the protocol of mean teacher, firstly, the labeled source samples are passed through student model for training. In particular, we employ Faster RCNN [30] as our object detection model. So the loss for training student model with the labeled source samples can be written as:

$$\mathcal{L}_{\text{det}}(\mathcal{B}^s, \mathcal{C}^s, \mathbf{I}^s) = \sum_{i=1}^{N_s} \mathcal{L}_{\text{rpn}}(\mathcal{B}_i^s, \mathbf{I}_i^s) + \mathcal{L}_{\text{roi}}(\mathcal{B}_i^s, \mathcal{C}_i^s, \mathbf{I}_i^s) \quad (1)$$

where \mathcal{L}_{rpn} is the loss for the Region Proposal Network(RPN) module which is used for proposal generation, and \mathcal{L}_{roi} is the loss for the prediction branch which performs bounding box regression and classification. More details can be found in [30].

Meanwhile, the unlabeled target samples are augmented with random cropping, padding and color jittering(i.e. brightness, contrast, hue and saturation augmentations). The augmented target samples are fed into teacher and student network, respectively, and then we take the highly confident predictions of teacher network to guide the student network via distillation. We denote the augmented target samples as $\tilde{\mathbf{I}}^t$ for student network, $\tilde{\mathbf{I}}^t$ for teacher network. The loss for distillation can be defined as:

$$\mathcal{L}_{\text{dist}}(\tilde{\mathbf{I}}^t, \hat{\mathbf{I}}^t) = \mathcal{L}_{\text{det}}(\mathcal{T}_B(\tilde{\mathbf{I}}^t), \mathcal{T}_C(\tilde{\mathbf{I}}^t), \hat{\mathbf{I}}^t) \quad (2)$$

where $\mathcal{T}_B(\tilde{\mathbf{I}}^t)$ and $\mathcal{T}_C(\tilde{\mathbf{I}}^t)$ are the confidently predicted bounding box coordinates and object classes from the teacher network on the augmented image $\tilde{\mathbf{I}}^t$, and \mathcal{L}_{det} is the Faster RCNN loss defined in Eq. (1).

Finally, the overall loss of the mean teacher can be obtained by putting together those two losses,

$$\mathcal{L} = \mathcal{L}_{\text{det}}(\mathcal{B}^s, \mathcal{C}^s, \mathbf{I}^s) + \lambda \mathcal{L}_{\text{dist}}(\tilde{\mathbf{I}}^t, \hat{\mathbf{I}}^t), \quad (3)$$

where λ is a trade-off parameter.

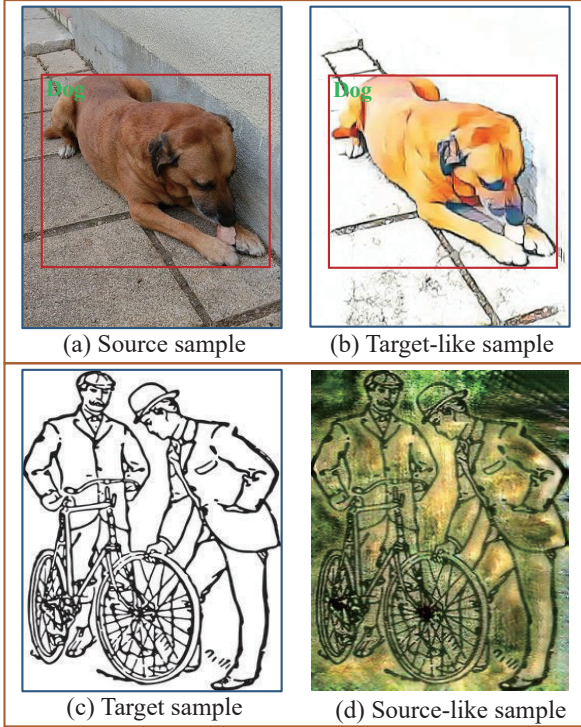


Figure 2: Examples of translated images. (a) and (c) are respectively a source example image from the PASCAL VOC dataset [6], and a target example from image from the Clipart1k dataset [16]. (b) is the target-like image by translating the source image (a) into the target style, and (d) is the source-like image by translating the target image (c) into the source style.

3.3. Investigating the Model Bias in Mean Teacher

Although the mean teacher can improve the robustness of predictions on target domain, it is inevitable that learned models will eventually be biased towards the source domain, as the supervision substantially comes from labeled source samples. As a result, in the distillation process, the prediction on the unlabeled target images produced by teacher network could be deficient. This issue might be relatively minor in classification task. However, in object detection, minor biases in localization may cause a considerable difference in feature pooling and therefore class prediction, and thus leads to inferior guidance to the student model.

To verify this, we conduct an experiment on the mean teacher models trained in the aforementioned way on several cross domain object detection datasets. In particular, we aim to investigate whether the teacher model is biased to the source domain, by comparing its performance on source and target samples. To ensure a fair comparison, we use unpaired image-to-image translation by CycleGAN[48] to produce a source-like image for each tar-

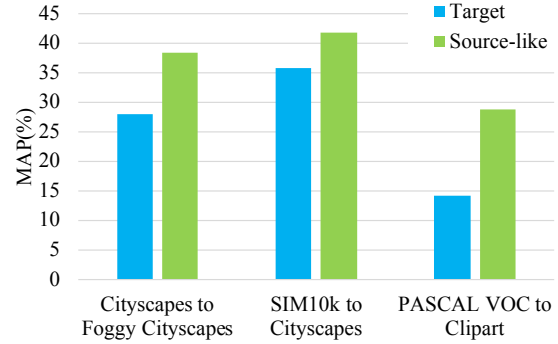


Figure 3: Evaluation of teacher models in mean teacher on target images and source-like images in different cross domain object detection scenarios. Mean Average precision (mAP) are used as the comparison metric. It can be observed the teacher models produces significant better detection results on source-like images, which clearly indicates the models are biased towards the source domain.

get image. An example of the source-like image on PASCAL VOC→Clipart1k is shown in Fig. 2(d). We then feed the target samples and the translated source-like samples into the teacher model, and evaluate their detection performance, respectively.

The average precisions (APs) of the teacher models for two versions of samples on different datasets are plotted in Fig. 3. We observe that the APs of teacher models on source-like samples generally outperform their APs on target samples. This clearly confirms our hypothesis that the teacher model is biased towards the source domain.

3.4. Healing the Model Bias in Mean Teacher

3.4.1 Healing the Teacher Model Bias

Motivated by the above observation, we propose to remodel the mean teacher model by pixel-level adaptation. Instead of using only target samples for distillation, we perform a *cross domain distillation* by using paired images $(\mathbf{I}^t, \mathbf{P}^t)$, where \mathbf{P}^t is the source-like version of the target image \mathbf{I}^t . As illustrated in Fig. 4, for each distillation iteration, we feed the source-like image \mathbf{P}^t to the teacher network, and the target image \mathbf{I}^t to the student network. In this way, the teacher network is expected to produce more precise predictions, thus being able to provide better guidance to the student network. Meanwhile, the student network is optimized over the original target samples for the distillation loss, which encourages its favor of target data. Thus, the original distillation loss in Eq. (2) is modified as,

$$\mathcal{L}_{dist}(\tilde{\mathbf{P}}^t, \hat{\mathbf{I}}^t) = \mathcal{L}_{det}(\mathcal{T}_B(\tilde{\mathbf{P}}^t), \mathcal{T}_C(\tilde{\mathbf{P}}^t), \hat{\mathbf{I}}^t) \quad (4)$$

where $\tilde{\mathbf{P}}^t$ is augmented from \mathbf{P}^t with small perturbations.

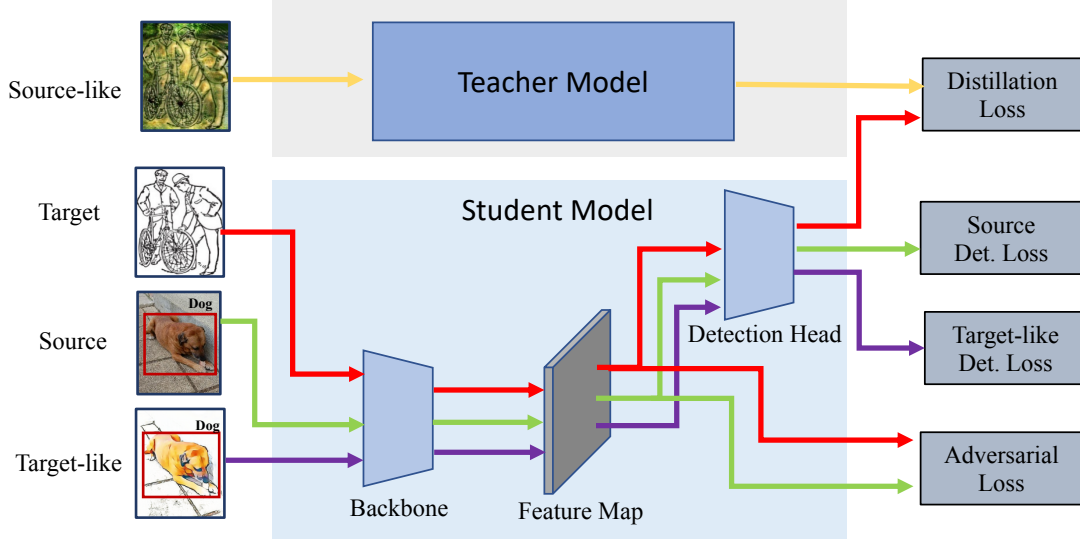


Figure 4: An overview of our proposed Unbiased Mean Teacher model. In each mini-batch, four types of images are used, source-like images, target images, target-like images, and source images. The source images with annotations are used to optimize the object detection loss of the student model (*i.e.*, Source Det. Loss); the source-like images and target images are respectively fed into the teacher and student network to perform the cross domain distillation(*i.e.*, Distillation Loss); the target-like images are used as additional training samples to train the student model(*i.e.*, Target-like Det. Loss); and finally, the source and target samples are used to perform feature-level adversarial training to learn domain-invariant features(*i.e.*, Adversarial Loss). These training routes are performed jointly in an end-to-end manner.

3.4.2 Healing The Student Model Bias

As the teacher model is a moving average of the student model, the bias of teacher model essentially comes from the student model. Therefore we also aim to reduce the model bias from the side of student model. Towards the goal, we translate the source images into target-like images. Then the target-like images are used to train the student network, in addition to the supervision from the original source samples. Similarly as in generating source-like images, we use Cyclegan a target-like version image \mathbf{P}^s for each source image \mathbf{I}^s (An example of target-like image is shown in Fig. 2(b)). As the image translation process does not change groundtruth label(*i.e.*, bounding boxes), we use the same label information for target-like images. In this way, the target-like images can encourage the student model to be more favorable of the target domain data, and thus to reduce the bias towards source data. The loss for target-like images can be written as:

$$\mathcal{L}_{\text{det}}(\mathcal{B}^s, \mathcal{C}^s, \mathbf{P}^s) = \sum_{i=1}^{N_s} \mathcal{L}_{\text{rpn}}(\mathcal{B}_i^s, \mathbf{P}_i^s) + \mathcal{L}_{\text{roi}}(\mathcal{B}_i^s, \mathcal{C}_i^s; \mathbf{P}_i^s) \quad (5)$$

which has the same form with the loss in Eq. (1), only replacing \mathbf{I}^s with \mathbf{P}^s .

3.4.3 Towards Domain Invariant Feature Learning

To further reduce the model bias of student model, we additionally apply a domain discrepancy loss to the student model for learning domain-invariant representation. Particularly, we employ the adversarial training strategy and take the adversarial training loss in the recent work SWDA [32] as an example due to its excellent performance on cross domain object detection. However, other techniques like [5, 8, 9, 25, 39] can also be incorporated into our model, and we leave this for future study.

Specifically, in SWDA the adversarial training component optimizes two losses on different feature-level. For the local feature, it designs strong element-wise feature map alignment module. For the global feature map, a weak alignment module is used to focus the adversarial loss on globally similar images and puts less attention on aligning globally dissimilar images. The feature-level adaptation loss can be written as:

$$\mathcal{L}_{\text{feat}}(\mathbf{I}^s, \mathbf{I}^t) = \mathcal{L}_{\text{local}}(\mathbf{I}, d) + \mathcal{L}_{\text{global}}(\mathbf{I}, d) \quad (6)$$

where $\mathcal{L}_{\text{local}}$ and $\mathcal{L}_{\text{global}}$ are respectively the local and global adversarial loss, $d \in \{0, 1\}$ is the domain label with 0 being source and 1 being target, and \mathbf{I} represent either a source or target image. More details of this adversarial loss can be found in [32].

Table 1: The average precision (AP, in %) on all classes from different methods for cross domain object detection on the Clipart1k test set for **PASCAL VOC**→**Clipart1k** adaptation. UMT_S , UMT_{SC} , UMT_{SCA} are special cases of our UMT models (see Section 4.1 for detailed explanation). SWDA* is the reproduced result using their released codes following our protocol, while SWDA is their reported results which also uses the target test set as unlabeled data for adaptation.

Method	aero	bicycle	bird	boat	bottle	bus	car	cat	chair	cow	table	dog	hrs	bike	prsn	plnt	sheep	sofa	train	tv	MAP
Source	11.9	31.8	27.7	23.7	30.4	44.3	27.9	17.3	32.7	37.3	13.5	13.0	28.4	54.1	56.6	30.1	32.9	6.5	35.5	25.9	29.1
DM[20]	25.8	63.2	24.5	42.4	47.9	43.1	37.5	9.1	47.0	46.7	26.8	24.9	48.1	78.7	63.0	45.0	21.3	36.1	52.3	53.4	41.8
SCL[37]	44.7	50.0	33.6	27.4	42.2	55.6	38.3	19.2	37.9	69.0	30.1	26.3	34.4	67.3	61.0	47.9	21.4	26.3	50.1	47.3	41.5
SWDA*	29.3	56.6	32.5	31.3	37.1	43.4	36.8	5.9	38.6	30.1	26.0	8.0	49.3	54.7	58.2	50.0	24.9	22.6	39.2	31.8	35.3
SWDA	26.2	48.5	32.6	33.7	38.5	54.3	37.1	18.6	34.8	58.3	17.0	12.5	33.8	65.5	61.6	52.0	9.3	24.9	54.1	49.1	38.1
UMT_S	30.9	51.8	27.2	28.0	31.4	59.0	34.2	10.0	35.1	19.6	15.8	9.3	41.6	54.4	52.6	40.3	22.7	28.8	37.8	41.4	33.6
UMT_{SC}	40.1	69.3	26.8	29.0	24.9	39.4	42.7	8.6	39.8	63.0	14.9	18.8	43.6	66.1	63.0	40.7	31.7	8.7	27.5	53.0	37.6
UMT_{SCA}	39.5	60.0	30.5	39.7	37.5	56.0	42.7	11.1	49.6	59.5	21.0	29.2	49.5	71.9	66.4	48.0	21.2	13.5	38.8	50.4	41.8
UMT	41.5	61.6	30.9	34.8	23.7	62.3	51.4	5.8	49.3	66.0	23.4	22.4	47.5	81.3	70.6	48.6	25.8	26.0	38.7	41.8	42.7
Oracle	33.3	47.6	43.1	38.0	24.5	82.0	57.4	22.9	48.4	49.2	37.9	46.4	41.1	54.0	73.7	39.5	36.7	19.1	53.2	52.9	45.0

3.4.4 The Overall Model

We illustrate the overall architecture of our Unbiased Mean Teacher in Fig. 4. The source-like and target-like data are generated offline. Then the model is trained jointly by optimizing all losses in an end-to-end manner. The overall training objective can be written as

$$\begin{aligned} \mathcal{L} = & \mathcal{L}_{\text{det}}(\mathcal{B}^s, \mathcal{C}^s, \mathbf{I}^s) + \mathcal{L}_{\text{det}}(\mathcal{B}^s, \mathcal{C}^s, \mathbf{P}^s) \\ & + \lambda \mathcal{L}_{\text{dist}}(\tilde{\mathbf{P}}^t, \hat{\mathbf{I}}^t) + \eta \mathcal{L}_{\text{feat}}(\mathbf{I}^s, \mathbf{I}^t) \end{aligned} \quad (7)$$

where the loss terms are respectively the detection loss on source samples defined in Eq. (1), the detection loss on target-like samples defined in Eq. (5), the cross domain distillation loss defined in Eq. (4), and the adversarial loss defined in Eq. (6), and λ and η are trade-off parameters.

4. Experiments

To validate the effectiveness of our approach, we compare with state-of-the-arts methods for cross domain object detection on benchmark datasets with three different types of domain shifts, including 1) real images to artistic images, 2) normal weather to adverse weather, 3) synthetic images to real images.

As a common practice, we adopt the protocol of unsupervised cross domain object detection in [5]. Full annotations including the bounding boxes and the corresponding classes labels of objects are available for the source domain training data, while the target domain only contains unlabeled images. Moreover, we can access only the unlabeled train set in the target domain, while the target domain test set is strictly held out during the training phase.

Implementation Details: Following [5, 32], we take the Faster RCNN [30] model as the base object detection model for our Unbiased Mean Teacher approach. The

Table 2: The average precision (AP, in %) on all classes from different methods for cross domain object detection on the Watercolor2k test set for **PASCAL VOC**→**Watercolor2k** adaptation. UMT_S , UMT_{SC} , UMT_{SCA} are special cases of our UMT models (see Section 4.1 for detailed explanation).

Method	bike	bird	car	cat	dog	person	MAP
Source	75.7	50.2	50.1	30.1	28.9	58.7	48.9
DM[20]	-	-	-	-	-	-	52.0
SCL[37]	82.2	55.1	51.8	39.6	38.4	64.0	55.2
SWDA[32]	82.3	55.9	46.5	32.7	35.5	66.7	53.3
UMT_S	76.2	53.4	46.2	39.3	34.9	71.5	53.6
UMT_{SC}	79.7	49.5	50.1	45.5	30.6	69.8	54.2
UMT_{SCA}	86.6	51.3	52.6	42.1	33.5	67.5	55.6
UMT	83.0	55.2	47.2	42.8	46.5	66.7	56.9
oracle	49.8	50.6	40.2	38.9	53.3	69.4	50.4

ResNet-101 [14] or VGG16 [38] model pre-trained on ImageNet [21] is used as the backbone for the Faster RCNN model. Following the implementation of Faster RCNN with ROI-alignment [46, 12], we rescale all images by setting the shorter side of the image to 600 while keeping the image aspect ratios.

For the mean teacher and our model, unless otherwise stated, we set the trade-off parameter $\lambda = 0.1$ for all the experiments. We train the student network with a learning rate of 0.001 for the first 50k iterations and schedule linear decay for the learning rate to 0.0001 for the next 30k iterations. Each batch consists of four image samples: source, target, source-like and target-like. The weight smooth coefficient parameter α of the exponential moving average for the teacher model is set to 0.99. Other experimental hyper-

Table 3: The average precision (AP, in %) on all classes from different methods for cross domain object detection on the validation set of Foggy Cityscapes for **Cityscapes**→**Foggy Cityscapes** adaptation. UMT_S , UMT_{SC} , UMT_{SCA} are special cases of our UMT models (see Section 4.1 for detailed explanation).

Method	bus	bicycle	car	mcycle	person	rider	train	truck	MAP
Source	24.7	29.0	27.2	16.4	24.3	31.5	9.1	12.1	21.8
DA-Faster[5]	35.3	27.1	40.5	20.0	25.0	31.0	20.2	22.1	27.6
PF[35]	-	-	-	-	-	-	-	-	28.9
SCDA[49]	39	33.6	48.5	28	33.5	38.0	23.3	26.5	33.8
DM[20]	38.4	32.2	44.3	28.4	30.8	40.5	34.5	27.2	34.6
MAF[15]	39.9	33.9	43.9	29.2	28.2	39.5	33.3	23.8	34.0
WD[45]	39.9	34.4	44.2	25.4	30.2	42.0	26.5	22.2	33.1
SCL[37]	41.8	36.2	44.8	33.6	31.6	44.0	40.7	30.4	37.9
MTOR[1]	38.6	35.6	44.0	28.3	30.6	41.4	40.6	21.9	35.1
SWDA[32]	36.2	35.3	43.5	30.0	29.9	42.3	32.6	24.5	34.3
UMT_S	30.1	31.3	36.1	22.4	27.9	38.2	20.2	21.5	28.5
UMT_{SC}	43.4	38.0	50.6	33.7	33.4	45.9	36.4	31.9	39.2
UMT_{SCA}	48.2	38.9	49.8	33.0	33.8	47.3	42.1	30.0	40.4
UMT	51.9	38.2	51.1	33.9	34.2	48.8	42.5	30.8	41.4
Oracle	50.0	36.2	49.7	34.7	33.2	45.9	37.4	35.6	40.3

parameters settings in our model follow the setup in [32].

4.1. Real to Artistic Adaptation

Datasets: In this experiment, we test our model with domain shift between the real image domain and artistic image domain. Following [32, 37], we combine the PASCAL VOC 2007 and PASCAL VOC 2012 datasets as the source domain, and use the Clipart1k and Watercolor2k datasets as target domains, respectively. The Clipart1k dataset contains 1,000 images from the same 20 classes as the PASCAL VOC dataset, which is split equally into a training set and a test set, containing 500 images each. We use the training set as the unlabeled target domain samples for domain adaptation in the training phase, and the test set are held out for evaluation. The Watercolor2k consists of 2,000 images from 6 classes in common with the PASCAL VOC dataset. Similarly, we use 1,000 images of as the target unlabeled training data for training models, and the remaining 1,000 images are held out for testing.

We include the results from state-of-the-art methods DM [20], SWDA [32] and the recently proposed SCL [37] for comparison. Besides, we report the oracle result by training a Faster RCNN model using the same images with target domain but with the ground truth annotations, which can be viewed as a reference for the upperbound adaptation performance. All methods are built on the Faster RCNN model, where ImageNet pre-trained ResNet101[14] is used as the backbone network.

Results: We report the average precision (AP) of each class as well as the mean AP over all classes in Table 1 and Table 2 for object detection on the Clipart1k and Wa-

tercolor2k datasets, respectively.

To understand the individual impact of the proposed components, we include several special versions of our UMT model for ablation study as follows: 1) UMT_S is the simple mean teacher model by optimizing the loss in Eq. (3); 2) UMT_{SC} is the mean teacher model with our cross domain distillation strategy as described in Section 3.4.1; and 3) UMT_{SCA} is the mean teacher model with both our cross domain distillation strategy in Section 3.4.1 and using the target-like images to augment the training set for the student model as described in Section 3.4.2.

We take the Clipart1k dataset as an example to explain the experimental results. In particular, the simple MT model UMT_S obtain a mean AP of 33.6%, which outperforms result of 29.1% from the source only baseline. This proves that the mean teacher model could help to improve the robustness of object detection model against data variance considerably. However, the improvement is not as significant as other state-of-the-art methods like DM, SWDA, and SCL, possibly due to the model bias problem as analysed in Section 3.3. By using the cross domain distillation the result is boosted to 37.6% (*i.e.*, UMT_{SC}), which is further improved to 41.8% (*i.e.*, UMT_{SCA}) with additionally using the target-like augmentation strategy. Note that the result of UMT_{SC} is already on par with the state-of-the-art result on this dataset (*i.e.*, DM), which clearly demonstrates the effectiveness of our strategies for handling the model biases in mean teacher. By further applying the domain invariant feature learning, our finally UMT model reaches 42.7%, which gives the new state-of-the-art performance for cross domain object detection on the Clipart1k dataset. The above obser-

vations are similar for the Watercolor2k dataset.

4.2. Adaptation in Inverse Weather

Datasets: In this experiment, we follow the setting in [5]. The training set of the Cityscapes dataset is used as the source domain, and the Foggy Cityscapes dataset [33] is used as the target domain. The Cityscapes dataset is collected from the urban street scene captured in 50 cities. The dataset contains 2,975 images in train set and 500 images in validation set. The Foggy Cityscapes is a synthetic foggy scene dataset rendered using the images and depth maps from Cityscapes, which therefore has the same data split as the Cityscapes dataset, *i.e.* a training set of 2,975 images a validation set of 500 images. We take labeled Cityscapes train set images and unlabeled Foggy Cityscapes train set images in our experiment, and report the evaluated results on the validation set of Foggy Cityscapes. Although there exists one-to-one correspondence between images in Cityscapes and Foggy Cityscapes datasets, we do not leverage such information in unsupervised domain adaptation.

Besides the baselines compared in last experiment, we further include DA-Faster [5], PF [35], SCDA [49], MAF [15], WD [45], and MTOR [1] for comparison. The setup for special cases of our UMT approach and the oracle method is the same as those in the previous experiment. All methods are built on Faster RCNN, where the VGG16 [38] pre-trained on ImageNet [21] is used as the backbone.

Results: Object detection in foggy scene images is extremely challenging due to the low visibility caused by the foggy weather. The current best state-of-the-art result on this dataset is 37.9% from the recently released work SCL [37]. However, the special case of our approach UMT_{SC} which using mean teacher with cross domain distillation already outperforms SCL with a mean AP of 39.2%. This again validates the effectiveness of the cross domain distillation strategy for improving the mean teacher model for cross domain object detection. Our final UMT model shows improved performance in all classes compared to SCL, and reaches a mean AP of 41.4%. Interestingly, this result exceeds the oracle result on this dataset, showing that the clear weather images with high visibility are useful for boosting the limits the object detection in the adverse foggy weather with low visibility, without requiring any annotations on those low visibility images.

4.3. Synthetic to Real

Datasets: Following [5], the SIM10k dataset [17] is used as the source domain, and the Cityscapes dataset is used as the target domain. The SIM10K dataset contains 10,000 images of the computer-rendered driving scene from the Grand Theft Auto(GTAV) game. The training set of Cityscapes is used the target training samples, and the validation set is used for evaluation.

Table 4: The average precision (AP, in %) of different methods for cross domain object detection on the validation set of Cityscapes for **SIM10K**→**Cityscapes** adaptation. UMT_S , UMT_{SC} , UMT_{SCA} are special cases of our UMT models (see Section 4.1 for detailed explanation).

Method	AP on car
Source	34.3
SCDA[49]	43.0
SCL[37]	42.6
SWDA[32]	40.1
MAF[15]	41.1
WD[45]	40.6
UMT_S	40.8
UMT_{SC}	42.0
UMT_{SCA}	42.6
UMT	43.1
Oracle	53.0

Results: Similarly as in the experiment for adverse weather, we use ImageNet pertained model as the backbone for our approach, and compare with existing state-of-the-arts using the same setting.

The AP on detecting cars for different approaches are reported in Table 4. Similarly as in the previous experiments, we observe that our UMT approach gradually improves the MT model by addressing its model bias with different strategies. Our final model also achieves the new state-of-the-art AP of 43.1% on this dataset using VGG-16 as the backbone, which again demonstrates the effectiveness of our proposed approach.

5. Conclusion

In this work, we have presented a new model named as Unbiased Mean Teacher for cross domain object detection. We address the challenge that object detection models are often vulnerable to data variance, especially in the domain scenarios. Our model is based on the mean teacher model. Motivated by our analysis on the model bias towards source data, we designed three highly effective strategies to remedy the bias. In particular, we firstly propose a new cross domain distillation to maximally exploit the expertise of the teacher model. Then, we further augment the training samples for the student model with pixel-level adaptation to reduce its model bias. Lastly, the feature level adversarial training is incorporated for learning domain-invariant representation. Extensive experiments are conducted on multiple benchmark datasets, where our proposed model surpasses the existing state-of-the-art models by large margins, which clearly demonstrates the effectiveness of our proposed approach.

References

[1] Qi Cai, Yingwei Pan, Chong-Wah Ngo, Xinmei Tian, Lingyu Duan, and Ting Yao. Exploring object relation in mean teacher for cross-domain detection. In *Proceedings of the IEEE Conference on Computer Vision and Pattern Recognition*, pages 11457–11466, 2019.

[2] Zhaowei Cai and Nuno Vasconcelos. Cascade r-cnn: Delving into high quality object detection. In *Proceedings of the IEEE conference on computer vision and pattern recognition*, pages 6154–6162, 2018.

[3] Fabio Maria Cariucci, Lorenzo Porzi, Barbara Caputo, Elisa Ricci, and Samuel Rota Bulò. Autodial: Automatic domain alignment layers. In *2017 IEEE International Conference on Computer Vision (ICCV)*, pages 5077–5085. IEEE, 2017.

[4] Yuhua Chen, Wen Li, Xiaoran Chen, and Luc Van Gool. Learning semantic segmentation from synthetic data: A geometrically guided input-output adaptation approach. In *Proceedings of the IEEE Conference on Computer Vision and Pattern Recognition*, pages 1841–1850, 2019.

[5] Yuhua Chen, Wen Li, Christos Sakaridis, Dengxin Dai, and Luc Van Gool. Domain adaptive faster r-cnn for object detection in the wild. In *CVPR*, 2018.

[6] Mark Everingham, Luc Van Gool, Christopher KI Williams, John Winn, and Andrew Zisserman. The pascal visual object classes (voc) challenge. *International journal of computer vision*, 88(2):303–338, 2010.

[7] Geoffrey French, Michal Mackiewicz, and Mark Fisher. Self-ensembling for visual domain adaptation. *arXiv preprint arXiv:1706.05208*, 2017.

[8] Yaroslav Ganin and Victor Lempitsky. Unsupervised domain adaptation by backpropagation. *arXiv preprint arXiv:1409.7495*, 2014.

[9] Yaroslav Ganin, Evgeniya Ustinova, Hana Ajakan, Pascal Germain, Hugo Larochelle, François Laviolette, Mario Marchand, and Victor Lempitsky. Domain-adversarial training of neural networks. *The Journal of Machine Learning Research*, 17(1):2096–2030, 2016.

[10] Ross Girshick. Fast r-cnn. In *Proceedings of the IEEE international conference on computer vision*, pages 1440–1448, 2015.

[11] Ross Girshick, Jeff Donahue, Trevor Darrell, and Jitendra Malik. Rich feature hierarchies for accurate object detection and semantic segmentation. In *Proceedings of the IEEE conference on computer vision and pattern recognition*, pages 580–587, 2014.

[12] Kaiming He, Georgia Gkioxari, Piotr Dollár, and Ross Girshick. Mask r-cnn. In *Proceedings of the IEEE international conference on computer vision*, pages 2961–2969, 2017.

[13] Kaiming He, Xiangyu Zhang, Shaoqing Ren, and Jian Sun. Spatial pyramid pooling in deep convolutional networks for visual recognition. *IEEE transactions on pattern analysis and machine intelligence*, 37(9):1904–1916, 2015.

[14] Kaiming He, Xiangyu Zhang, Shaoqing Ren, and Jian Sun. Deep residual learning for image recognition. In *Proceedings of the IEEE conference on computer vision and pattern recognition*, pages 770–778, 2016.

[15] Zhenwei He and Lei Zhang. Multi-adversarial faster-rcnn for unrestricted object detection. In *Proceedings of the IEEE International Conference on Computer Vision*, pages 6668–6677, 2019.

[16] Naoto Inoue, Ryosuke Furuta, Toshihiko Yamasaki, and Kiyoharu Aizawa. Cross-domain weakly-supervised object detection through progressive domain adaptation. In *Proceedings of the IEEE conference on computer vision and pattern recognition*, pages 5001–5009, 2018.

[17] Matthew Johnson-Roberson, Charles Barto, Rounak Mehta, Sharath Nittur Sridhar, Karl Rosaen, and Ram Vasudevan. Driving in the matrix: Can virtual worlds replace human-generated annotations for real world tasks? *arXiv preprint arXiv:1610.01983*, 2016.

[18] Mehran Khodabandeh, Arash Vahdat, Mani Ranjbar, and William G Macready. A robust learning approach to domain adaptive object detection. *arXiv preprint arXiv:1904.02361*, 2019.

[19] Seunghyeon Kim, Jaehoon Choi, Taekyung Kim, and Changick Kim. Self-training and adversarial background regularization for unsupervised domain adaptive one-stage object detection. In *Proceedings of the IEEE International Conference on Computer Vision*, pages 6092–6101, 2019.

[20] Taekyung Kim, Minki Jeong, Seunghyeon Kim, Seokeon Choi, and Changick Kim. Diversify and match: A domain adaptive representation learning paradigm for object detection. In *Proceedings of the IEEE Conference on Computer Vision and Pattern Recognition*, pages 12456–12465, 2019.

[21] Alex Krizhevsky, Ilya Sutskever, and Geoffrey E Hinton. Imagenet classification with deep convolutional neural networks. In *Advances in neural information processing systems*, pages 1097–1105, 2012.

[22] Tsung-Yi Lin, Piotr Dollár, Ross Girshick, Kaiming He, Bharath Hariharan, and Serge Belongie. Feature pyramid networks for object detection. In *Proceedings of the IEEE conference on computer vision and pattern recognition*, pages 2117–2125, 2017.

[23] Tsung-Yi Lin, Michael Maire, Serge Belongie, James Hays, Pietro Perona, Deva Ramanan, Piotr Dollár, and C Lawrence Zitnick. Microsoft coco: Common objects in context. In *European conference on computer vision*, pages 740–755. Springer, 2014.

[24] Wei Liu, Dragomir Anguelov, Dumitru Erhan, Christian Szegedy, Scott Reed, Cheng-Yang Fu, and Alexander C Berg. Ssd: Single shot multibox detector. In *European conference on computer vision*, pages 21–37. Springer, 2016.

[25] Mingsheng Long, Yue Cao, Jianmin Wang, and Michael I Jordan. Learning transferable features with deep adaptation networks. *arXiv preprint arXiv:1502.02791*, 2015.

[26] Mingsheng Long, Han Zhu, Jianmin Wang, and Michael I Jordan. Unsupervised domain adaptation with residual transfer networks. In *Advances in Neural Information Processing Systems*, pages 136–144, 2016.

[27] Mingsheng Long, Han Zhu, Jianmin Wang, and Michael I Jordan. Deep transfer learning with joint adaptation networks. In *Proceedings of the 34th International Conference on Machine Learning-Volume 70*, pages 2208–2217. JMLR.org, 2017.

[28] Joseph Redmon, Santosh Divvala, Ross Girshick, and Ali Farhadi. You only look once: Unified, real-time object detection. In *Proceedings of the IEEE conference on computer vision and pattern recognition*, pages 779–788, 2016.

[29] Joseph Redmon and Ali Farhadi. Yolo9000: better, faster, stronger. In *Proceedings of the IEEE conference on computer vision and pattern recognition*, pages 7263–7271, 2017.

[30] Shaoqing Ren, Kaiming He, Ross Girshick, and Jian Sun. Faster r-cnn: Towards real-time object detection with region proposal networks. In *Advances in neural information processing systems*, pages 91–99, 2015.

[31] Aruni RoyChowdhury, Prithvijit Chakrabarty, Ashish Singh, SouYoung Jin, Huaizu Jiang, Liangliang Cao, and Erik Learned-Miller. Automatic adaptation of object detectors to new domains using self-training. In *Proceedings of the IEEE Conference on Computer Vision and Pattern Recognition*, pages 780–790, 2019.

[32] Kuniaki Saito, Yoshitaka Ushiku, Tatsuya Harada, and Kate Saenko. Strong-weak distribution alignment for adaptive object detection. In *CVPR*, 2019.

[33] Christos Sakaridis, Dengxin Dai, and Luc Van Gool. Semantic foggy scene understanding with synthetic data. *International Journal of Computer Vision*, 126(9):973–992, 2018.

[34] Swami Sankaranarayanan, Yogesh Balaji, Carlos D Castillo, and Rama Chellappa. Generate to adapt: Aligning domains using generative adversarial networks. In *Proceedings of the IEEE Conference on Computer Vision and Pattern Recognition*, pages 8503–8512, 2018.

[35] Yuhu Shan, Wen Feng Lu, and Chee Meng Chew. Pixel and feature level based domain adaptation for object detection in autonomous driving. *Neurocomputing*, 367:31–38, 2019.

[36] Zhiqiang Shen, Zhuang Liu, Jianguo Li, Yu-Gang Jiang, Yurong Chen, and Xiangyang Xue. Dsod: Learning deeply supervised object detectors from scratch. In *Proceedings of the IEEE International Conference on Computer Vision*, pages 1919–1927, 2017.

[37] Zhiqiang Shen, Harsh Maheshwari, Weichen Yao, and Marios Savvides. Scl: Towards accurate domain adaptive object detection via gradient detach based stacked complementary losses. *arXiv preprint arXiv:1911.02559*, 2019.

[38] Karen Simonyan and Andrew Zisserman. Very deep convolutional networks for large-scale image recognition. *arXiv preprint arXiv:1409.1556*, 2014.

[39] Baochen Sun and Kate Saenko. Deep coral: Correlation alignment for deep domain adaptation. In *European Conference on Computer Vision*, pages 443–450. Springer, 2016.

[40] Antti Tarvainen and Harri Valpola. Mean teachers are better role models: Weight-averaged consistency targets improve semi-supervised deep learning results. In *Advances in neural information processing systems*, pages 1195–1204, 2017.

[41] Eric Tzeng, Kaylee Burns, Kate Saenko, and Trevor Darrell. Splat: Semantic pixel-level adaptation transforms for detection. *arXiv preprint arXiv:1812.00929*, 2018.

[42] Eric Tzeng, Judy Hoffman, Kate Saenko, and Trevor Darrell. Adversarial discriminative domain adaptation. In *Proceedings of the IEEE Conference on Computer Vision and Pattern Recognition*, pages 7167–7176, 2017.

[43] Jasper RR Uijlings, Koen EA Van De Sande, Theo Gevers, and Arnold WM Smeulders. Selective search for object recognition. *International journal of computer vision*, 104(2):154–171, 2013.

[44] Rongchang Xie, Fei Yu, Jiachao Wang, Yizhou Wang, and Li Zhang. Multi-level domain adaptive learning for cross-domain detection. In *Proceedings of the IEEE International Conference on Computer Vision Workshops*, pages 0–0, 2019.

[45] Pengcheng Xu, Prudhvi Gurram, Gene Whipps, and Rama Chellappa. Wasserstein distance based domain adaptation for object detection. *arXiv preprint arXiv:1909.08675*, 2019.

[46] Jianwei Yang, Jiasen Lu, Dhruv Batra, and Devi Parikh. A faster pytorch implementation of faster r-cnn. <https://github.com/jwyang/faster-rcnn.pytorch>, 2017.

[47] Weichen Zhang, Wanli Ouyang, Wen Li, and Dong Xu. Collaborative and adversarial network for unsupervised domain adaptation. In *Proceedings of the IEEE Conference on Computer Vision and Pattern Recognition*, pages 3801–3809, 2018.

[48] Jun-Yan Zhu, Taesung Park, Phillip Isola, and Alexei A Efros. Unpaired image-to-image translation using cycle-consistent adversarial networks. In *Proceedings of the IEEE international conference on computer vision*, pages 2223–2232, 2017.

[49] Xinge Zhu, Jiangmiao Pang, Ceyuan Yang, Jianping Shi, and Dahua Lin. Adapting object detectors via selective cross-domain alignment. In *Proceedings of the IEEE Conference on Computer Vision and Pattern Recognition*, pages 687–696, 2019.